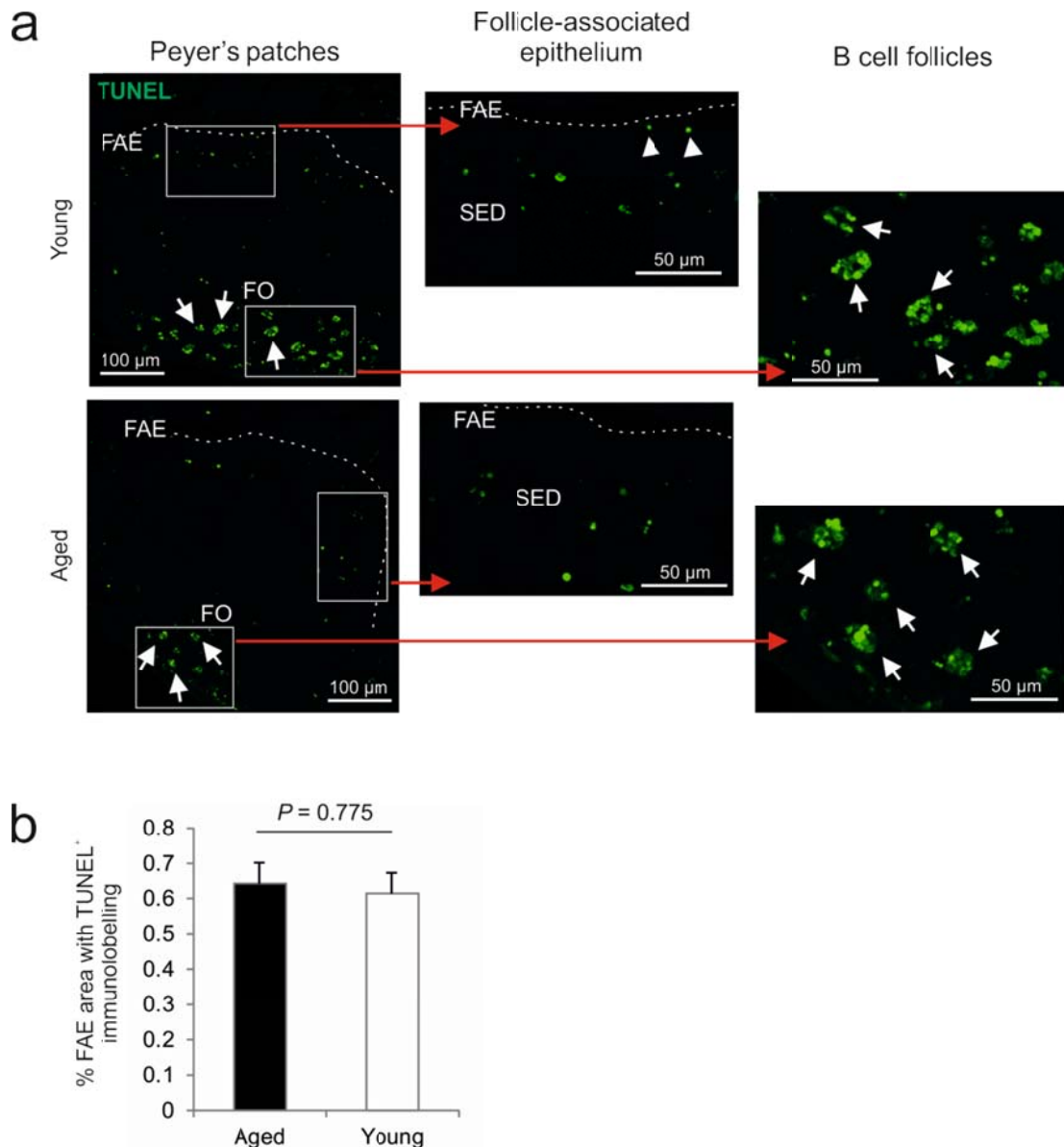


Supplementary Figure 1. Effect of ageing on cell proliferation in Peyer's patches.

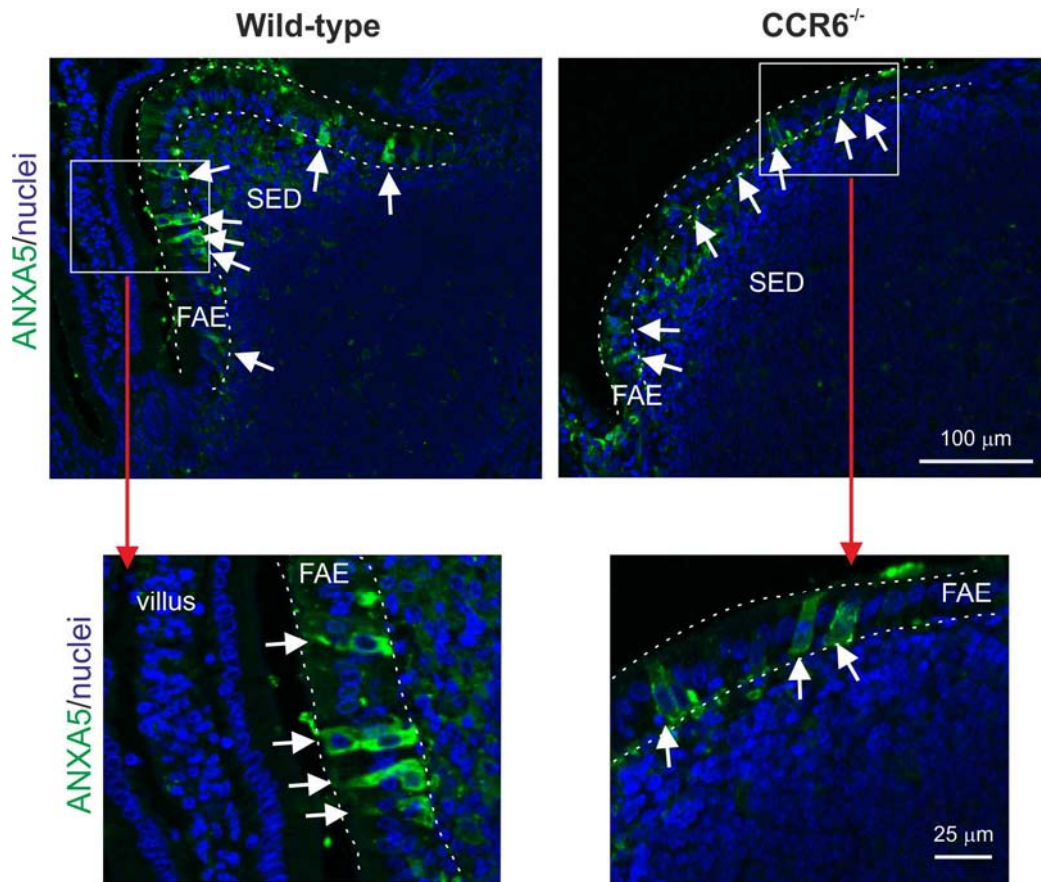
(a) Proliferating cells in the Peyer's patches of young and aged mice were detected

by IHC (Ki-67⁺ cells, green). Whereas there was a dramatic reduction in the number of proliferating (Ki-67⁺) cells in the Peyer's patch follicles (FO) of aged mice, no difference was observed in the dome-associated crypts (arrows). The boxed areas of dome-associated crypts in each of the left-hand images are shown on the right-hand side at higher magnification. Left-hand images; broken line indicates the luminal surface of the FAE. Right-hand images; broken line indicates the basolateral surface of the dome-associated crypts. (b) Morphometric analysis of the number (upper panels) and density (lower panels) of proliferating cells (Ki67⁺ cells) in the follicles (left-hand panels) and dome-associated crypts (right-hand panels) of Peyer's patches from young and aged mice. Data are derived from 3-5 Peyer's patches from 4 mice from each group.

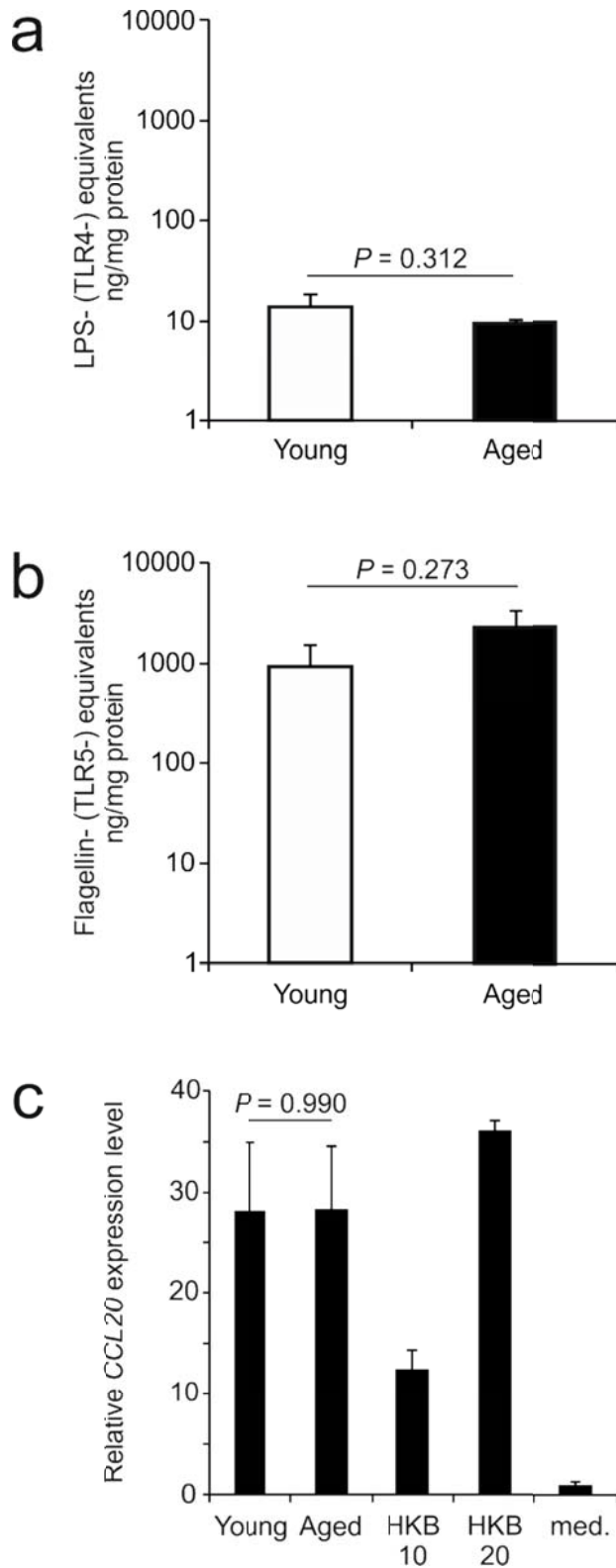


Supplementary Figure 2. Effect of ageing on apoptosis in Peyer's patches. (a) As anticipated, in the B cell follicles (FO in main image) numerous tingible body macrophages (arrows) contained large numbers of apoptotic cells (TUNEL⁺ cells, green). Apoptotic cells were rare in the FAE (arrow-heads). SED, sub-epithelial dome. Boxed areas in main panels (left-hand images) are presented at higher magnification (middle and right-hand images). Broken line indicates the luminal surface of the FAE. (b) No significant difference in the density of the TUNEL⁺ immunostaining was observed in the FAE of Peyer's patches from young and aged

mice ($P = 0.775$). Data are derived from 3-6 Peyer's patches from 4 young mice and 9 aged mice.

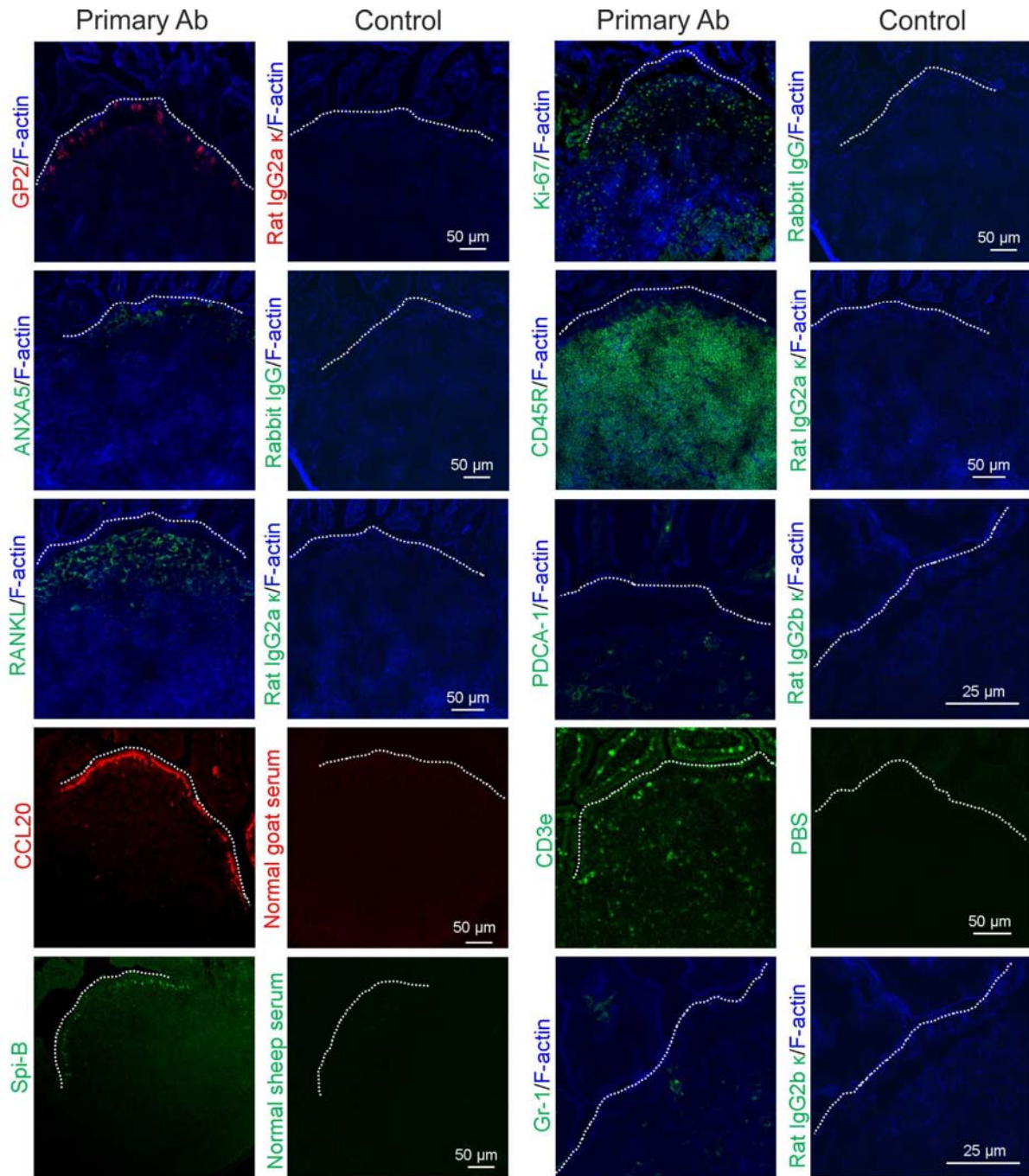


Supplementary Figure 3. CCR6-deficiency does not affect the expression of ANXA5 in the FAE. IHC analysis of the expression of ANXA5 (green) by M cells in the FAE of wild-type (control) and CCR6^{-/-} mice. Nuclei were detected using the DNA-intercalating dye DAPI (blue). Arrows, ANXA5⁺ cells in the FAE. The boxed areas of the FAE in the main panels (upper images) are presented at higher magnification (lower images). Broken lines indicate the boundaries of the FAE. SED, sub-epithelial dome.



Supplementary Figure 4. Effect of ageing on the relative abundance of soluble PAMP in the intestine. (a&b) The relative abundance of PAMP-equivalents specific for TLR4 (a) and TLR5 (b) were measured in individual SFE preparations from young

and aged mice using TLR-transfected HEK-293 cells as described in the Materials and Methods. PAMP abundance in SFE is presented as ng PAMP/mg protein. (c) SFE derived from young or aged mice induced similar levels of *CCL20* mRNA expression by *in vitro*-cultivated Caco-2 cells. Data were normalized to the expression level of *ACTB*. Data are presented as the fold change relative to the normalized expression level in unstimulated (medium alone) cells. HKB, whole heat-killed faecal bacteria. Med., medium alone (control). All data are derived from duplicate SFE samples from 6 young and 6 aged mice, and two independent experiments.



Supplementary Figure 5 Images of Peyer's patches showing typical examples of the immunostaining obtained with the primary Ab used in this study (first and third columns) and their corresponding negative controls (second and fourth columns, respectively). Broken line indicates the luminal surface of the FAE.